Effect of Ferric Oxyhydroxide Grain Coatings on the Transport of Bacteriophage PRD1 and *Cryptosporidium parvum* Oocysts in Saturated Porous Media[†]

R. A. ABUDALO,[‡] Y. G. BOGATSU,[‡]
J. N. RYAN,*,[‡] R. W. HARVEY,[§]
D. W. METGE,[§] AND M. ELIMELECH[||]

Department of Civil, Environmental, and Architectural Engineering, University of Colorado, 428 UCB, Boulder, Colorado 80309, Water Resources Division, U. S. Geological Survey, 3215 Marine Street, Boulder, Colorado 80303, and Environmental Engineering Program, Department of Chemical Engineering, Yale University, New Haven, Connecticut 06520

To test the effect of geochemical heterogeneity on microorganism transport in saturated porous media, we measured the removal of two microorganisms, the bacteriophage PRD1 and oocysts of the protozoan parasite *Cryptosporidium parvum*, in flow-through columns of quartz sand coated by different amounts of a ferric oxyhydroxide. The experiments were conducted over ranges of ferric oxyhydroxide coating fraction of $\lambda = 0-0.12$ for PRD1 and from $\lambda = 0-0.32$ for the oocysts at pH 5.6−5.8 and 10^{-4} M ionic strength. To determine the effect of pH on the transport of the oocysts, experiments were also conducted over a pH range of 5.7−10.0 at a coating fraction of $\lambda = 0.04$. Collision (attachment) efficiencies increased as the fraction of ferric oxyhydroxide coated quartz sand increased, from $\alpha = 0.0071$ to 0.13 over $\lambda = 0-0.12$ for PRD1 and from $\alpha = 0.059$ to 0.75 over $\lambda = 0-0.32$ for the oocysts. Increasing the pH from 5.7 to 10.0 resulted in a decrease in the oocyst collision efficiency as the pH exceeded the expected point of zero charge of the ferric oxyhydroxide coatings. The collision efficiencies correlated very well with the fraction of quartz sand coated by the ferric oxyhydroxide for PRD1 but not as well for the oocysts.

Introduction

To mitigate the public health concern of pathogenic microorganisms in surface waters used as potable water supplies and to reduce disinfection requirements, water utilities are considering the use of riverbank filtration (*1−4*). Predicting microorganism removal during riverbank filtration is difficult because alluvial valley sediments are typically physically and geochemically heterogeneous. One form of geochemical heterogeneity in natural sediments is the different surface

charge of minerals that make up the sediments (*5*). For many sediments, much of the surface charge heterogeneity can be attributed to the distribution of ferric oxyhydroxide coatings on the grain surfaces (*6−9*).

At pH values between the points of zero charge of ferric oxyhydroxide minerals (pH_{pzc} 7.5−9) and quartz (pH_{pzc} 2−3), ferric oxyhydroxides are positively charged and quartz grains are negatively charged. Microorganisms exhibit negative surface charge over most of this pH range, so they will readily attach to the ferric oxyhydroxide coatings and avoid deposition on the quartz surfaces. Johnson et al. (*10*) first demonstrated the importance of this "patch-wise" surface charge heterogeneity with negatively charged silica colloids and ferric oxyhydroxide coated quartz sand. Using silica colloids and aminosilane-coated quartz sand, Elimelech et al. (*11*) further refined the mechanism. Elimelech et al. (*11*) found a direct relationship between the collision efficiency (α), the probability of a collision between a particle and grain resulting in attachment of the particle, and the fraction of positively charged surface on the grains (λ)

$$\alpha = \alpha_f\lambda + \alpha_u(1 - \lambda) \approx \lambda \tag{1}$$

where α is the overall collision efficiency, α_f is the collision efficiency for favorable deposition ($\alpha_f \approx 1$), and α_u is the collision efficiency for unfavorable deposition ($\alpha_u \ll \alpha_f$).

Laboratory and field experiments with microorganisms have shown that ferric oxyhydroxide coatings are important in the removal of microorganisms in saturated porous media (*9, 12−19*), even in the presence of organic matter and phosphate, which can block microorganism attachment (*20, 21*). But none of these experiments have measured microorganism removal over a range of surface coating fractions. To do this, we examined the transport of the bacteriophage (bacteria-specific virus) PRD1 and oocysts of a protozoan intestinal parasite, *Cryptosporidium parvum*, in sand columns packed with different mixtures of ferric oxyhydroxide coated and uncoated quartz sand. For most of the experiments, the ferric oxyhydroxide coatings were expected to act as favorable deposition sites for the microorganisms and the quartz as unfavorable deposition sites. Our goal was to test the relationship between collision efficiency and the fraction of ferric oxyhydroxide surface coatings. We also increased the solution pH to reverse the surface charge of the ferric oxyhydroxide coatings and highlight the importance of surface charge heterogeneity on microorganism deposition.

Materials and Methods

Virus. The bacteriophage PRD1 was used as the virus for these experiments. PRD1 has frequently been used as a surrogate for examining the transport behavior of pathogenic viruses (*22*). PRD1 has a diameter of 62 nm. Above a pH of about 3, PRD1 is negatively charged (*18, 23*). The bacteriophage was produced and assayed following techniques described in detail by Loveland et al. (*15*). The bacteriophages were suspended in the aqueous solution to be used in the column experiments at a concentration of about 10^9 virus mL^{-1}. The electrophoretic mobility of PRD1 was measured by laser Doppler microelectrophoresis (Particle Sizing Systems, 380 ZLS) over a pH range of 5.0−10.0 in 10^{-4} M NaCl at a concentration of about 10^{11} virus mL^{-1}. The electrophoretic mobilities were converted to zeta potentials using a tabulation of the O'Brien and White (*24*) solution of mobility equations.

***Cryptosporidium parvum* Oocysts.** Formalin-inactivated *Cryptosporidium parvum* oocysts were obtained from Sterling

Parasitology Laboratory (SPL) at the University of Arizona at Tucson. We used formalin-inactivated oocysts to allow the use of the same oocysts in an intermediate-scale aquifer tank experiment that could not be conducted in a biologically safe laboratory. Oocysts exhibit an isoelectric point (pH_{iep}) of about 3 (25–28). Inactivation by formalin (or by heat) does not significantly alter the pH_{iep} or zeta potential of oocysts at near neutral pH (29–31), but inactivation by formalin and heat did enhance oocyst deposition in a radial stagnation point flow system (31).

The oocysts were shed from a calf infected with the Iowa isolate of *Cryptosporidium parvum* (obtained from Dr. Harvey Moon, National Animal Disease Center, Ames, Iowa), purified at the SPL by discontinuous sucrose and cesium chloride centrifugation gradients (32), resuspended in a solution of 5% formaldehyde, 0.01% Tween 20, 0.85% NaCl, and three antibiotics (penicillin, 111 U mL^{-1}; streptomycin, 111 U mL^{-1}; gentamicin, 56 μg mL^{-1}), and stored at 4 °C. Before the column experiments, the oocysts were pelleted from the formalin solution by centrifugation (12 000g, 4 °C, 30 min) and resuspended in the aqueous solution to be used in the column experiments at a concentration of about 10^5 oocyst mL^{-1}. The oocysts were suspended in the aqueous solution at least 30 days before the transport experiments.

The oocysts were enumerated by epifluorescence microscopy. Samples containing oocysts were stained with 4,6-diamidino-2-phynylindole (DAPI; 0.1 mg L^{-1} solution, 15 min contact time), filtered with vacuum assistance (0.34 bar) onto black polycarbonate membranes (1.0 μm pore diameter, Osmonics), prepared with a cover slide and immersion oil, and counted manually using an epifluorescence microscope (Nikon Optiphot-2, 788× magnification, 350 nm excitation, 470 nm emission). At least 20 fields of view with 10 oocysts per field, or a maximum of 50 fields if fewer than 10 oocysts per field were present, were counted.

The average diameter of the oocysts was measured by immunofluorescent flow cytometry analysis (33, 34) of DAPI-stained oocysts. The flow cytometer (Biorad, HS Bryte) was calibrated using fluorescent microspheres. The buoyant density of the oocysts was measured using a Percoll I solution (1.131 g mL^{-1}, Sigma Chemical Co.) density gradient centrifugation (Sorvall RC-5B, 15 000g, 1 h, 20 °C) with marker beads (35). The electrophoretic mobility of the oocysts was measured by laser Doppler microelectrophoresis over a pH range of 3.3–10.1 in 10^{-4} M NaCl at a concentration of about 10^6 oocyst mL^{-1}.

Porous Media. For the PRD1 experiments, angular quartz sand was obtained from a commercial supplier (Aldrich Chemical Co., +70/−50 mesh, 0.21–0.30 mm). The median grain size was 0.25 mm, and the ratio of the PRD1 and grain diameters was 2.5×10^{-4}. For the oocyst experiments, larger, well-rounded quartz sand was obtained from a commercial supplier (Unimin Corp., 2095 sand) and mechanically dry-sieved (+20/−18 mesh) to retain a narrow size fraction (0.84–1.00 mm). The median grain size was 0.92 mm (Figure 1), and the ratio of the oocyst and grain diameters was 0.0039. This ratio is just below the ratio of oocyst and grain diameters for which straining was observed (0.005) for oocysts in quartz sand by Bradford and Bettahar (36). The sand fractions were acid-washed following the method of Redman et al. (37).

Some of the quartz sand was coated with ferric oxyhydroxide following a procedure similar to that used by Mills et al. (14) to produce the geochemically heterogeneous porous media. Examination of individual coated grains by thin sectioning and scanning electron microscopy (backscatter electron detection) showed that 75 ± 5% of the grain surfaces were covered by a relatively uniform layer of iron oxyhydroxide for both sand size fractions. Preparation of the geochemically heterogeneous porous media was done by mixing portions of the coated and uncoated sand to achieve
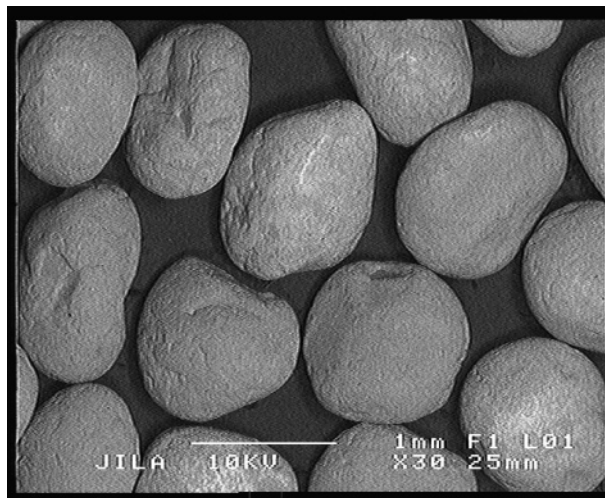

FIGURE 1. Scanning electron microscopy image of the 0.92 mm quartz sand (0.84–1.00 mm fraction) used in the oocyst column experiments (JEOL, JSM-6400; gold-coated sample, 10 kV accelerating voltage). The scale bar is 1 mm.

ferric oxyhydroxide coating surface coverage ranging from $\lambda = 0$ to 0.12 for the PRD1 experiments and $\lambda = 0$ to 0.32 for the oocyst experiments, where λ is the fraction of the quartz grain surfaces coated by ferric oxyhydroxide (11). The 75% surface coating fraction of the coated grains was accounted for in the mixing. The amounts of iron, aluminum, and manganese on the coated and uncoated sand were determined by a partial acid digestion (1.5 M HCl and 30% H_2O_2, 57 °C, 3 h; ref 38). The metal concentrations were measured in the digestion solutions by inductively coupled plasma-atomic emission spectrometry (ICP-AES; Applied Research Laboratories ARL-3410+).

Solutions. Solutions were prepared using high-purity water (greater than 18 MΩ cm resistivity; Millipore Milli-Q). The background solution for all column experiments was 10^{-4} M NaCl and pH 5.6–5.8. The solution pH was increased to as high as 10.0 for certain oocyst experiments by addition of 0.1 M NaOH solution. Nitrate (added as 10^{-4} M NaNO$_3$) was used as a conservative tracer and measured by ultraviolet absorption (220 nm wavelength) using a spectrophotometer (Spectronic/Unicam, Genesys 10).

Columns. The transport experiments were conducted in glass chromatography columns (1.5 cm diameter; 20.0 cm length and 13.4 mL pore volume for PRD1; 10.0 cm length and 6.7 mL pore volume for the oocysts) with polytetrafluoroethene end caps and polypropylene mesh (105 μm openings) on both ends of the column. The background solution was pumped to the column through polypropylene tubing by a piston pump (stainless steel, 500 mL volume, Isco 500D). Tracer solutions and microorganism suspensions were added to the background solution using a high performance liquid chromatography injector (stainless steel; Supelco Rheodyne) and injection loop (stainless steel, 2.0 mL volume for PRD1, 5.0 mL volume for oocysts). A fraction collector and glass test tubes were used to collect the column effluent.

To pack the columns, various ratios of coated and uncoated grains were mixed so that the coated grains were randomly distributed among the uncoated grains, although the randomness of the distribution of the coated grains does not matter (17, 39). The coated/uncoated mixture of grains was added to about 1–2 cm of standing water in the column (the background solution) in 1 cm lifts. The column was tapped to avoid trapping of air bubbles. Porosity was determined by the difference in mass between a saturated and dry-packed column and confirmed by analysis of the

tracer breakthrough. The average column porosity was 0.38 ± 0.02 for both the PRD1 and oocyst experiments. Before each experiment, several pore volumes of the background solution were pumped though the column until the pH and specific conductance of inlet and outlet solutions were the same.

The oocyst experiments were conducted at room temperature. The PRD1 experiments were conducted at 5.0 ± 0.5 °C to minimize inactivation by placing a loop of tubing (15 mL volume; about 1 h residence time), the injector, the column, and the fraction collector in a refrigerator. At this temperature, we estimate that inactivation of PRD1 in solution and attached to the mineral surfaces contributed to the removal of less than 2% of the PRD1 in the column. This estimate is based on an overall inactivation rate coefficient of 0.2 day^{-1} estimated by Schijven et al. (*40*) by inverse modeling of a PRD1 field transport experiment.

Experimental Procedures. For the PRD1 experiments, the pump was filled with the background electrolyte solution (10^{-4} M NaCl) and the injection loop was filled with the conservative tracer nitrate (added as 10^{-4} M NaNO$_3$) and the PRD1 suspension. The sodium nitrate and the PRD1 were co-injected as a single pulse. For the oocyst experiments, the tracer solution (2.5 × 10^{-3} M NaNO$_3$; pH 5.6−5.8) and the oocyst suspension in 10^{-4} M NaCl were injected as two separate pulses to use a higher tracer concentration and to provide more sample for oocyst measurement without increasing the volume of each fraction collector sample. Relatively small total numbers of PRD1 and oocysts were injected to maintain "clean-bed" deposition kinetics. The pH of the background solution and injectate for most of the experiments was 5.6−5.8. An additional set of oocyst experiments was conducted at higher pH (from 5.7 to 10.0) with a ferric oxyhydroxide coated sand of $\lambda = 0.04$. The $\lambda = 0.04$ porous medium was chosen for these experiments because the fraction of ferric oxyhydroxide surface coating is similar to that of the glacial outwash sediments that comprise the surficial aquifer on Cape Cod, Massachusetts (*18*). The pumping rates were set to produce pore velocities of 6.0 ± 0.1 m day^{-1} for PRD1 and 2.0 ± 0.1 m day^{-1} for the oocysts. For a porosity of 0.38, the Darcy, or approach, velocities were 2.3 m day^{-1} for PRD1 and 0.76 m day^{-1} for the oocsyts. At least three pore volumes of breakthrough were monitored for each experiment. Selected PRD1 and oocyst experiments were duplicated.

Breakthrough Analysis. The PRD1 and oocyst breakthrough data was used to determine the collision efficiency (α) with the following equation (*41*)

$$\alpha = -\frac{2}{3}\frac{d_c \ln \text{RB}}{(1-f)x_1\eta_0} \tag{2}$$

where d_c is the collector grain diameter, f is the porosity, x_1 is the column length, η_0 is the theoretical single collector contact efficiency calculated using the Tufenkji and Elimelech (*42*) equation using the parameters listed in Table 1, and RB is the cumulative fractional breakthrough

$$\text{RB} = \frac{N_{\text{eff}}}{N_{\text{inj}}} \tag{3}$$

where N_{eff} is the total number of microorganisms in the column effluent and N_{inj} is the total number of microorganisms in the injectate. This determination of the collision efficiency is valid for microorganism removal solely by physicochemical filtration.

Mass Balance. For the oocyst experiments, a mass balance was assessed for the column effluent, the quartz sand, and the column components. Oocysts on the sand were removed

TABLE 1. Parameters Used in the Calculation of Single Collector Contact Efficiency (*42*) and Collision Efficiency (α) for Bacteriophage PRD1 and *Cryptosporidium parvum* Oocysts[a]

parameter	PRD1	oocysts
grain diameter (mm)	0.25	0.92
porosity	0.38	0.38
particle diameter (μm)	0.062	3.6
particle density (g cm^{-3})	1.05	1.075
temperature (°C)	5	20
fluid approach velocity (m day^{-1})	2.3	0.76
fluid density (g cm^{-3})	1.000	0.998
fluid viscosity (kg m^{-1} s^{-1})	1.52 × 10^{-3}	1.00 × 10^{-3}
Hamaker constant (J)	6.5 × 10^{-21}	6.5 × 10^{-21}
column length (cm)	20	10

[a] The PRD1 density was estimated. The Hamaker constant value was deemed appropriate for a bacteria−quartz−water system by Kuznar and Elimelech (*31*).

by gentle disaggregation (suspension of the grains in the experimental solution) and vigorous shaking in a pH 10 solution (suspension of the grains for 30 min on a shaking table) to ensure complete release of the deposited oocysts. Oocysts on the column apparatus were removed by vigorous shaking in a pH 10 solution. Mass balances for the oocyst experiments averaged 98 ± 1.5% (Table 2). In two duplicate experiments, the polypropylene mesh on the influent end of the column removed 1.8 and 2.0% of the oocysts. These oocysts were deducted from the number of oocysts in the injectate (N_{inj}). Breakthrough results were not compensated for the loss of oocysts to other column components.

Results

Microorganism and Porous Media Characteristics. The average diameter of the oocysts was measured as 3.6 ± 0.3 μm (±1 standard deviation) by flow cytometry. Kuznar and Elimelech (*43*) measured a similar diameter (3.7 μm) for oocysts obtained from the same source using optical microscopy and image analysis. The buoyant density of the oocysts was measured as 1.075 ± 0.005 g cm^{-3} (±1 standard deviation) by Percoll density gradient centrifugation. Medema et al. (*44*) measured an oocyst density of 1.0454 g cm^{-3} using a similar technique. The zeta potential of PRD1 and *Cryptosporidium parvum* oocysts were negative over the pH range used in the column experiments (Figure 2). At pH 5.6−5.8, the pH of most of the experiments, the magnitude of the PRD1 zeta potential was about twice that of the oocysts. As pH increases from 6.0 to 10.1, the magnitude of the oocyst zeta potentials decreased slightly.

The acid-washing and combustion of the 0.92 mm sand removed about 99% of the iron content (Table 3), which left quartz sand with very low levels of iron and manganese impurities, similar to the 0.25 mm sand. Only about half of the aluminum in the 0.92 mm sand was removed by the acid-washing and combustion. For both sand fractions, the coating process resulted in about 1000 times more iron mass (and $\lambda = 0.75 ± 0.05$) on the coated quartz than on the uncoated quartz.

Microorganism Breakthrough Curves. For most of the PRD1 and oocyst breakthrough curves, the breakthrough of the microorganisms coincided closely with the breakthrough of the conservative tracer, nitrate (Figure 3). The mean ratio of the pore volumes at which breakthrough occurred for PRD1 and nitrate was 0.98 ± 0.08. For the oocysts and the nitrate, the mean ratio was 1.04 ± 0.10. Breakthrough was identified as the number of pore volumes at which the constituent concentration was at half the value of the maximum concentration measured for the breakthrough.

TABLE 2. Results of Mass Balance Checks for Experiments of Oocyst Transport through Uncoated Quartz Sand ($\lambda = 0$) Showing Oocyst Association with Quartz Sand and Column Components (with Materials and Oocyst Extraction Method)

| column contents or component	fraction of injected oocysts (%)	number of experiments
column effluent	73.5 ± 1.4	2
retained on quartz sand		3
(gentle disaggregation, background solution)	15.9 ± 0.8	
(vigorous shaking, pH 10 solution)	4.6 ± 1.2	2
injection loop	0.08 ± 0.01	2
(stainless steel; pH 10 solution)		
column mesh, influent end	1.9 ± 0.1	2
(polypropylene; pH 10 solution)		
column walls and end caps	0.59 ± 0.07	2
(glass; shaking in pH 10 solution)		
column mesh, effluent end	0.52 ± 0.13	2
(polypropylene; pH 10 solution)		
fraction collector sample tubes	0.88	1
(glass; pH 10 solution)		
total	98.0 ± 1.5	2
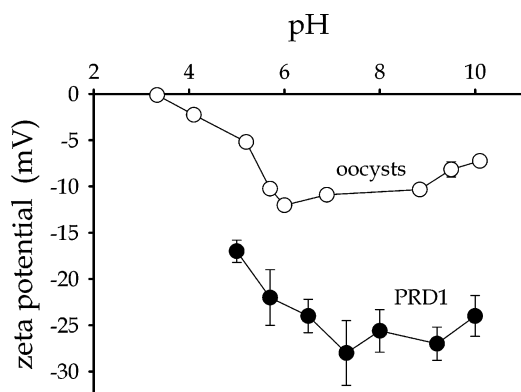
FIGURE 2. Zeta potential as a function of pH for bacteriophage PRD1 and formalin-inactivated *Cryptosporidium parvum* oocysts in 10^{-4} M NaCl as measured by laser Doppler microelectrophoresis. Sodium hydroxide and hydrochloric acid were used to adjust the pH.

Effect of Ferric Oxyhydroxide Coating on PRD1 Deposition. As the fraction of ferric oxyhydroxide coated quartz sand increased from $\lambda = 0$ to 0.12, the relative breakthrough of the bacteriophage PRD1 decreased from RB = 62.1 to 0.02% (Figure 4). The corresponding values of the collision efficiency increased from 0.0071 to 0.13.

Effect of Ferric Oxyhydroxide Coating on Oocyst Deposition. As the fraction of ferric oxyhydroxide coated quartz sand increased from $\lambda = 0$ to 0.32, the overall relative breakthrough of the *Cryptosporidium parvum* oocysts decreased from RB = 76.5 to 3.3% (Figure 5). The corresponding values of the collision efficiency increased from 0.059 to 0.75.

Effect of pH on Oocyst Deposition. The relative breakthrough of oocysts in the $\lambda = 0.04$ porous medium decreased at pH 8.0 and increased at pH 10.0 relative to the breakthrough at the other pH values tested (Figure 6). The corresponding values of the collision efficiency ranged from $\alpha = 0.32$ at pH 8.0 to $\alpha = 0.11$ at pH 10.0.

Discussion

Microorganism Characteristics. Both the PRD1 and the *Cryptosporidium parvum* oocysts were negatively charged under the conditions of the experiments. At high pH (9−10), the zeta potentials of both the PRD1 and the oocysts became slightly less negative. At these high pH values, the addition of sodium hydroxide and the uptake of carbon dioxide increase the ionic strength, and increases in ionic strength result in decreases in the absolute value of the zeta potential.

At the pH of most of the experiments (pH 5.6−5.8), the magnitude of the oocyst zeta potential is only about half that of the PRD1. Other researchers have measured similarly low negative zeta potentials for *Cryptosporidium parvum* oocysts (25−31). For PRD1, surface charge comes from the amino acids that make up the bacteriophage's protein capsid, which include aspartic acid, arginine, glutamic acid, lysine, histidine, and cysteine (45). For oocysts, surface charge comes from the amino acids that make up the oocyst wall, which include cysteine, proline, and histidine (46).

Effect of Ferric Oxyhydroxide Coating on PRD1 Deposition. The dependence of the PRD1 collision efficiencies (α) on the fraction of ferric oxyhydroxide surface coating (λ) closely matches the Elimelech et al. (11) relationship $\alpha \approx \lambda$ (Figure 4). For PRD1, the collision efficiency−surface coating fraction relationship is $\alpha = 1.02(\pm 0.08)\lambda + 0.0021(\pm 0.0049)$, $R^2 = 0.96$.

The assumptions that lead to good agreement between the PRD1 results and the $\alpha \approx \lambda$ relationship—that $\alpha_f \approx 1$ and $\alpha_u \ll \alpha_f$—appear to be satisfied. PRD1 is negatively charged (Figure 2), and the points of zero charge for various ferric oxyhydroxides range from 7.5 to 9.0 (47), so the ferric oxyhydroxide coating should be positively charged. Therefore, the collision efficiency for PRD1 deposition on the ferric oxyhydroxide coating should be $\alpha_f \approx 1$. The collision efficiency for PRD1 deposition on quartz is $\alpha_u = 0.0071$ as determined by the $\lambda = 0$ (pure quartz sand) column experiment, and if $\alpha_f \approx 1$, then $\alpha_u \ll \alpha_f$.

While the assumptions for the $\alpha \approx \lambda$ relationship are satisfied, the collision efficiencies measured at the lower values of λ are higher than those predicted by $\alpha \approx \lambda$ (Figure 4). The physicochemical filtration of PRD1 by the uncoated quartz is greater than that predicted by $\alpha \approx \lambda$ because PRD1 interaction with the quartz is not completely unfavorable—some deposition occurs. Some favorable deposition sites may still exist on the quartz owing to incomplete removal of surface impurities or surface roughness (11).

Effect of Ferric Oxyhydroxide Coating on Oocyst Deposition. The dependence of the *Cryptosporidium parvum* oocysts collision efficiencies (α) on the fraction of ferric oxyhydroxide surface coating (λ) does not closely match the

TABLE 3. Metal Concentrations for Partial Acid Digestions of the 0.25 mm Quartz Sand Used in the PRD1 Experiments and 0.92 mm Quartz Sand Used in the Oocyst Experiments

sand and treatment	Fe (mg kg^{-1})	Mn (mg kg^{-1})	Al (mg kg^{-1})
0.25 mm, after acid-washing and combustion	0.94	0.047	4.2
0.25 mm, ferric oxyhydroxide coated	990	1.9	4.5
0.92 mm, as received from supplier	43	1.0	5.9
0.92 mm, after acid-washing and combustion	0.45	0.017	2.6
0.92 mm, ferric oxyhydroxide coated	440	0.091	2.5
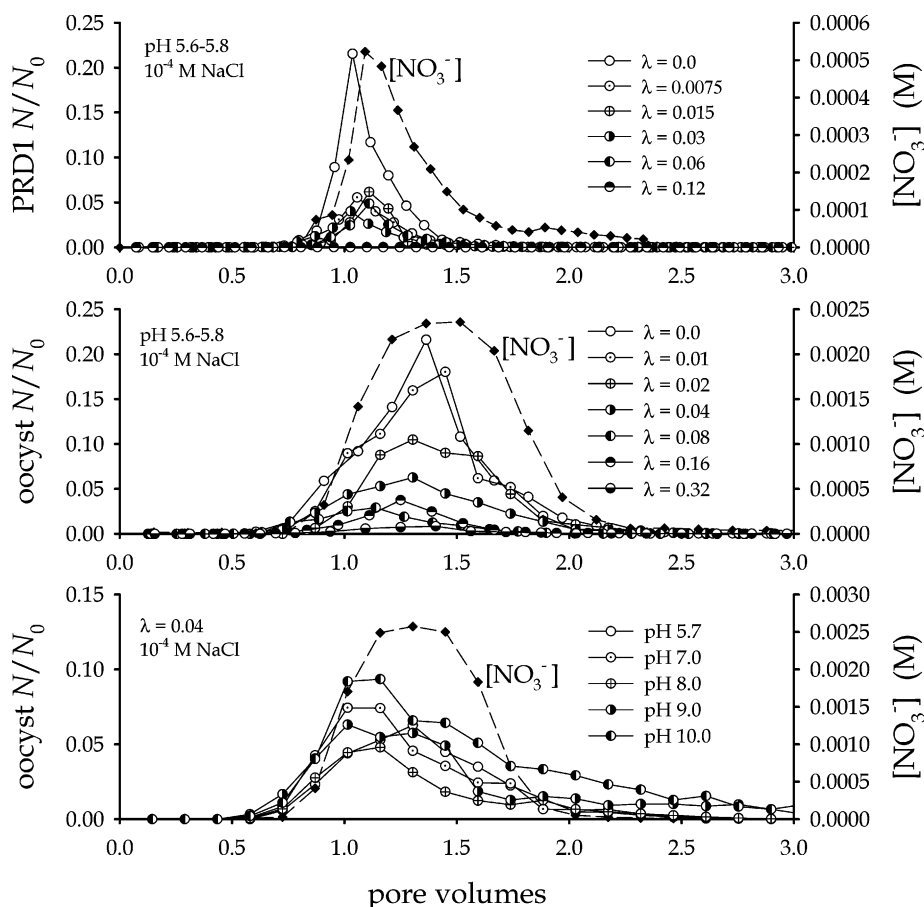
FIGURE 3. Breakthrough of nitrate, the conservative tracer, and bacteriophage PRD1 as a function of the surface ferric oxyhydroxide coating fraction (top), nitrate and *Cryptosporidium parvum* oocysts as a function of the surface ferric oxyhydroxide coating fraction (middle), and nitrate and *Cryptosporidium parvum* oocysts as a function of pH in quartz sand with $\lambda = 0.04$ ferric oxyhydroxide coating (bottom). Duplicate experiments are not shown.

relationship found by Elimelech et al. (*11*). A linear regression of the oocyst collision efficiency and the surface coating fraction yielded $\alpha = 2.1(\pm 0.3)\lambda + 0.15(\pm 0.04)$, $R^2 = 0.86$. The slope of this regression is about 2 times greater than that of the expected $\alpha \approx \lambda$ relationship.

At higher values of λ, the oocyst collision efficiencies are, on average, about 2 times greater than those predicted by the $\alpha \approx \lambda$ relationship. The discrepancy between collision efficiency and surface coating fraction may be caused by inaccuracy in the calculation of the single collector efficiency for oocysts—an error of a factor of 2 in the calculation of the single collector efficiency would not be surprising under these conditions. Calculating the single collector efficiency for the 62 nm PRD1 is subject to less error because Brownian diffusion is the only important collision mechanism. For the 3.6 μm oocysts, sedimentation, diffusion, and interception contribute significantly (sedimentation causes about 5 times more collisions than diffusion and about 10 times more collisions than interception), and the possibility for error in the single collector efficiency is greater. An error of a factor

of 2 in the calculation of the single collector efficiency would not be surprising under these conditions. Ideally, we would have conducted a column experiment at $\lambda = 1.00$ to measure the rate of "fast" oocyst deposition to entirely favorable surfaces instead of calculating the single collector efficiency (*10*, *11*), but the precipitation of ferric oxyhydroxide on the quartz grains resulted in coating of only 75% of the grain surfaces, so we could not conduct a $\lambda = 1.00$ experiment.

It is also possible that discrepancy between the measured and the expected collision efficiencies could be caused by reversible deposition of the oocysts on the quartz surfaces. If the oocysts are deposited reversibly and released in proximity to ferric oxyhydroxide coated surfaces, then oocysts may be retained on coated surfaces with which they would not have collided if they were not reversibly deposited on nearby quartz surfaces first. If deposition occurs on a coated surface without a collision, then the measured collision efficiency will be greater than that expected for a given coating fraction (λ). Reversible deposition can occur for colloids and microorganisms deposited in the secondary minimum of
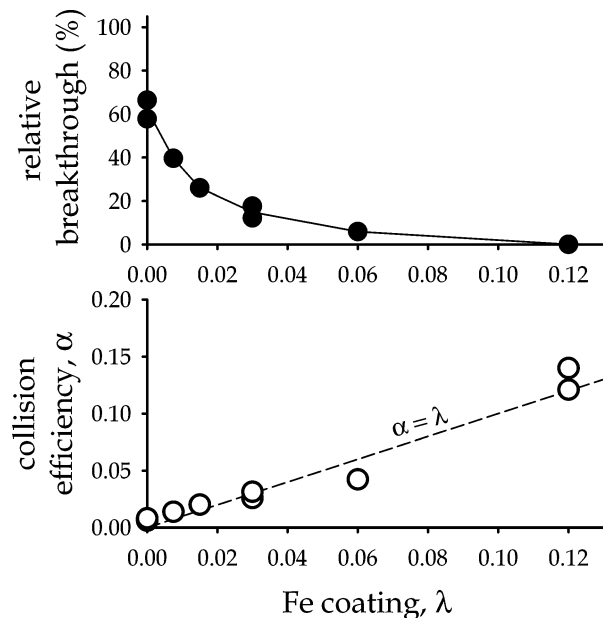
FIGURE 4. Relative breakthrough and collision efficiency (α) of the bacteriophage PRD1 as a function of the fraction of the ferric oxyhydroxide surface coating of the quartz sand (Fe coating, λ) at pH 5.6−5.8 and 1 × 10⁻⁴ M NaCl. The dashed line in the collision efficiency graph shows the expected α ≈ λ relationship (*11*).
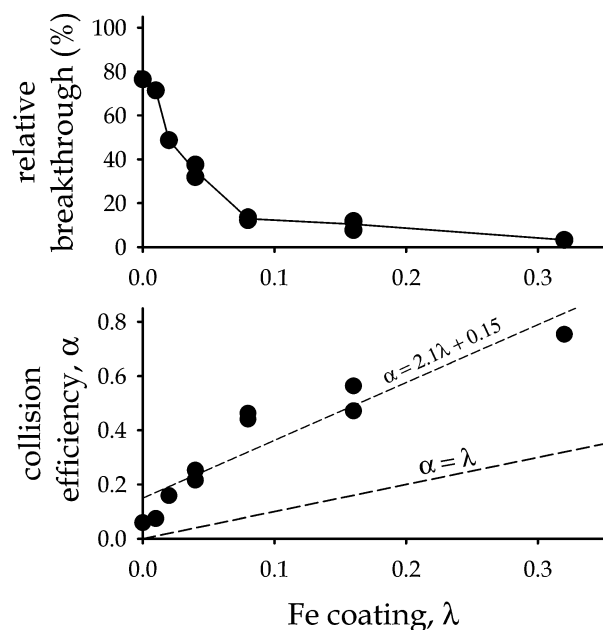

FIGURE 5. Relative breakthrough and collision efficiency (α) of *Cryptosporidium parvum* oocysts as a function of the fraction of the ferric oxyhydroxide surface coating of the quartz sand (Fe coating, λ) at pH 5.6−5.8 and 1 × 10⁻⁴ M NaCl. The dashed line in the collision efficiency graph shows the expected α ≈ λ relationship (*11*).

the Derjaguin−Landau−Verwey−Overbeek (DLVO; refs *48* and *49*) potential energy−distance profile (*43*, *50*, *51*), but DLVO calculations indicate that secondary minimum deposition is unlikely for oocysts at 10⁻⁴ M ionic strength.

Effect of pH on Oocyst Deposition. The dependence of *Cryptosporidium parvum* oocyst deposition on pH (Figure 6) validates a basic assumption about the role of ferric oxyhydroxide coatings in limiting microorganism transport— that the negatively charged microorganisms are readily deposited on positively charged ferric oxyhydroxide coatings. As the pH of the background solution increased to 10.0, the
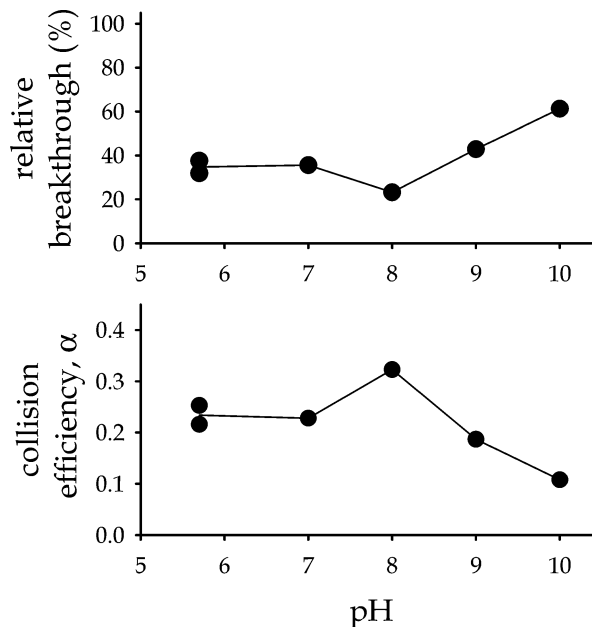

FIGURE 6. Measured relative breakthrough and collision efficiency (α) of *Cryptosporidium parvum* oocysts as a function of pH in a λ = 0.04 porous medium at 10⁻⁴ M NaCl.

relative breakthrough of the oocysts increased significantly. With a typical range of point of zero charge from 7.5 to 9.0 for ferric oxyhydroxides (*47*), the pH 10.0 solution probably caused a reversal of surface charge from positive to negative and a decrease in the overall collision efficiency for the oocysts. With negative charge on both the ferric oxyhydroxide coatings and the quartz, we might expect that deposition of the oocysts would be quite unfavorable (α ≪ 1), but like on the clean quartz, some oocyst deposition still occurs at pH 10.0 (40% of the injected oocysts, α = 0.11). We surmise that some oocyst deposition still occurs because the oocyst zeta potential remains low even at pH 10.0 (about −23 mV, Figure 2), and the ferric oxyhydroxide zeta potential would also be low because the solution pH is only 1−2 pH units above the expected point of zero charge. The most filtration occurred at pH 8.0, a pH at which the ferric oxyhydroxide surface charge would be close to zero and the zeta potential of the oocysts was decreasing in magnitude. These conditions may have led to the least repulsive interactions between the oocysts, the coatings, and the quartz surfaces.

Environmental Implications. The dependence of PRD1 deposition on the fraction of ferric oxyhydroxide coatings closely matches the expected α ≈ λ relationship (*11*), but the oocyst deposition does not. PRD1 deposition in porous media is relatively simple compared to oocyst deposition. For PRD1, the collisions leading to deposition occur primarily by Brownian diffusion because PRD1 is so small (diameter 62 nm). For the oocysts, the collisions occur by sedimentation, diffusion, and interception. The unexpected lack of a linear correlation between oocyst collision efficiency and the fraction of ferric oxyhydroxide coatings suggests that the kinetics of physicochemical filtration have not been accurately quantified for larger colloids.

Efforts have been made to incorporate the effects of surface charge heterogeneity into models of microbe transport in porous media (*52*), but the application of such models is limited by characterization of the surface coating in natural sediments. Even for simple natural sediments for which our model ferric oxyhydroxide coated quartz is a good approximation, measuring the surface coating fraction (λ) requires petrographic or scanning electron microscopy. Relationships between the surface coating fraction and the

amount of extractable iron have not been developed, and such relationships would be highly sensitive to the sediment grain size and the iron extraction technique. The simplicity of dividing mineral surfaces into sites of favorable and unfavorable deposition would not be appropriate for natural sediments containing minerals with a range of surface charges. Finally, the effects of organic matter and other anions that adsorb to positively charged mineral surfaces complicate the application of a simple surface charge heterogeneity model (20, 21). One simplification that aids in the application of the surface charge heterogeneity model is that the distribution of the surface coating favoring deposition is not important, only the fraction coated for the entire transport path (17, 39).

Acknowledgments

Literature Cited

(1) Gollnitz, W. D.; Clancy, J. L.; Garner, S. C. Reduction of microscopic particulates by aquifers. *J. Am. Water Works Assoc.* **1997**, *89*, 84−93.

(2) Schijven, J. F.; Berger, P.; Miettinen, I. Removal of pathogens, surrogates, indicators and toxins using bank filtration. In *Riverbank Filtration: Improving Source Water Quality*; Ray, C., Ed.; Kluwer Academic: Dordrecht, The Netherlands, 2002; Chapter 3.1.

(3) Tufenkji, N.; Ryan, J. N.; Elimelech, M. The promise of bank filtration. *Environ. Sci. Technol.* **2002**, *36*, A422−A428.

(4) Berger, P. Removal of *Cryptosporidium* using bank filtration. In *Riverbank Filtration: Understanding Contaminant Biogeochemistry and Pathogen Removal*; Ray, C., Bourg, A. C. M., Laszlo, F., Eds.; Kluwer Academic Publishers: Dordrecht, The Netherlands, 2003.

(5) Song, L.; Johnson, P. R.; Elimelech, M. Kinetics of colloid deposition onto heterogeneously charged surfaces in porous media. *Environ. Sci. Technol.* **1994**, *28*, 1164−1171.

(6) Ryan, J. N.; Gschwend, P. M. Effect of iron diagenesis on the transport of colloidal clay in an unconfined sand aquifer. *Geochim. Cosmochim. Acta* **1992**, *56*, 1507−1521.

(7) Coston, J. A.; Fuller, C. C.; Davis, J. A. Pb^{2+} and Zn^{2+} adsorption by a natural aluminum- and iron-bearing surface coating on an aquifer sand. *Geochim. Cosmochim. Acta* **1995**, *59*, 3535−3547.

(8) Penn, R. L.; Zhu, C.; Xu, H.; Veblen, D. R. Iron oxide coatings on sand grains from the Atlantic coastal plain: High-resolution transmission electron microscopy characterization. *Geology* **2003**, *29*, 843−946.

(9) Dong, H.; Onstott, T. C.; DeFlaun, M. F.; Fuller, M. E.; Schiebe, T. D.; Streger, S.; Rothmel, R. K.; Mailloux, B. J. Relative dominance of physical versus chemical effects on the transport of adhesion-deficient bacteria in intact cores from South Oyster, Virginia *Environ. Sci. Technol.* **2002**, *36*, 891−900.

(10) Johnson, P. R.; Sun, N.; Elimelech, M. Colloid transport in geochemically heterogeneous porous media: Modeling and measurements. *Environ. Sci. Technol.* **1996**, *30*, 3284−3293.

(11) Elimelech, M.; Nagai, M.; Ko, C.-H.; Ryan, J. N. Relative insignificance of mineral grain zeta potential to colloid transport in geochemically heterogeneous porous media. *Environ. Sci. Technol.* **2000**, *34*, 2143−2148.

(12) Fuhs, G. W.; Chen, M.; Sturman, L. S.; Moore, R. S. Virus adsorption to mineral surfaces is reduced by microbial overgrowth and organic coatings. *Microb. Ecol.* **1985**, *11*, 25−39.

(13) Scholl, M. A.; Harvey, R. W. Laboratory investigations on the role of sediment surface and groundwater chemistry in transport of bacteria through a contaminated sandy aquifer. *Environ. Sci. Technol.* **1992**, *26*, 1410−1417.

(14) Mills, A. L.; Herman, J. S.; Hornberger, G. M.; DeJesús, T. H. Effect of solution ionic strength and iron coatings on minerals grains on the sorption of bacterial cells to quartz sand. *Appl. Environ. Microbiol.* **1994**, *60*, 3300−3306.

(15) Loveland, J. P.; Ryan, J. N.; Amy, G. L.; Harvey, R. W. The reversibility of virus attachment to mineral surfaces. *Colloids Surf., A* **1996**, *107*, 205−221.

(16) Johnson, W. P.; Logan, B. E. Enhanced transport of bacteria in porous media by sediment-phase and aqueous-phase organic matter. *Water Res.* **1996**, *30*, 923−931.

(17) Knapp, E. P.; Herman, J. S.; Hornberger, G. M.; Mills, A. L. The effect of distribution of iron-oxyhydroxide grain coatings on the transport of bacterial cells in porous media. *Environ. Geol.* **1998**, *33*, 243−248.

(18) Ryan, J. N.; Elimelech, M.; Ard, R. A.; Harvey, R. W.; Johnson, P. R. Bacteriophage PRD1 and silica colloid transport and recovery in an iron oxide-coated sand aquifer. *Environ. Sci. Technol.* **1999**, *33*, 63−73.

(19) Bolster, C. H.; Mills, A. L.; Hornberger, G. M.; Herman, J. S. Effect of surface coatings, grain size, and ionic strength on the maximum attainable coverage of bacteria on sand surfaces. *J. Contam. Hydrol.* **2001**, *50*, 287−305.

(20) Pieper, A. P.; Ryan, J. N.; Harvey, R. W.; Amy, G. L.; Illangasekare, T. H.; Metge, D. W. Transport and recovery of bacteriophage PRD1 in a sand and gravel aquifer: Effect of sewage-derived organic matter. *Environ. Sci. Technol.* **1997**, *31*, 1163−1170.

(21) Dong, H.; Onstott, T. C.; Ko, C.-H.; Hollingsworth, A. D.; Brown, D. G.; Mailloux, B. J. Theoretical prediction of collision efficiency between adhesion-deficient bacteria and sediment grain surface. *Colloids Surf., B* **2002**, *24*, 229−245.

(22) Harvey, R. W.; Ryan, J. N. Use of PRD1 bacteriophage in groundwater viral transport, inactivation, and attachment studies. *FEMS Microbiol. Ecol.* **2004**, *49*, 3−16.

(23) Bales, R. C.; Hinkle, S. R.; Kroeger, T. W.; Stocking, K.; Gerba, C. P. Bacteriophage adsorption during transport through porous media: Chemical perturbations and reversibility. *Environ. Sci. Technol.* **1991**, *25*, 2088−2095.

(24) O'Brien, R. W.; White, L. R. The electrophoretic mobility of a spherical colloidal particle. *J. Chem. Soc., Faraday Trans. 2* **1978**, *74*, 1607−1626.

(25) Ongerth, J. E.; Pecoraro, J. P. Electrophoretic mobility of *Cryptosporidium* oocysts and *Giardia* cysts. *J. Environ. Eng.* **1996**, *122*, 228−231.

(26) Karaman, M. E.; Pashley, R. M.; Bustamante, H.; Shanker, S. R. Microelectrophoresis of *Cryptosporidium parvum* oocysts in aqueous solutions of inorganic and surfactant cations. *Colloids Surf., A* **1999**, *146*, 217−225.

(27) Considine, R. F.; Drummond, C. J. Surface roughness and surface force measurement: A comparison of electrostatic potentials derived from atomic force microscopy and electrophoretic mobility measurements. *Langmuir* **2001**, *17*, 7777−7783.

(28) Hsu, B.-M.; Huang, C. Influence of ionic strength and pH on hydrophobicity and zeta potential of *Giardia* and *Cryptosporidium*. *Colloids Surf., A* **2002**, *201*, 201−206.

(29) Considine, R. F.; Dixon, D. R.; Drummond, C. J. Oocysts of *Cryptosporidium parvum* and model sand surfaces in aqueous solutions: An atomic force microscope (AFM) study. *Water Res.* **2002**, *36*, 3421−3428.

(30) Butkus, M. A.; Bays, J. T.; Labare, M. P. Influence of surface characteristics on the stability of *Cryptosporidium parvum* oocysts. *Appl. Environ. Microbiol.* **2003**, *69*, 3819−3825.

(31) Kuznar, Z. A.; Elimelech, M. Role of surface proteins in the deposition kinetics of *Cryptosporidium parvum* oocysts. *Langmuir* **2005**, *21*, 710−716.

(32) Brush, C. F.; Walter, M. F.; Anguish, L. J.; Ghiorse, W. C. Influence of pretreatment and experimental conditions on electrophoretic mobility and hydrophobicity of *Cryptosporidium parvum* oocysts. *Appl. Environ. Microbiol.* **1998**, *64*, 4439−4445.

(33) Vesey, G.; Hutton, P.; Champion, A.; Ashbolt, N.; Williams, K. L.; Warton, A.; Veal, D. Application of flow cytometric methods for the routine detection of *Cryptosporidium* and *Giardia* in water. *Cytometry* **1994**, *16*, 1−6.

(34) Delaunay, A.; Gargala, G.; Li, X.; Favennec, L.; Ballet, J. J. Quantitative flow cytometric evaluation of maximal *Cryptosporidium parvum* oocyst infectivity in a neonate mouse model. *Appl. Environ. Microbiol.* **2000**, *66*, 4315−4317.

(35) Harvey, R. W.; Metge, D. W.; Kinner, N.; Mayberry, N. Physiological considerations in applying laboratory-determined buoyant densities to predictions of bacterial and protozoan

transport in groundwater: Results of in-situ and laboratory tests. *Environ. Sci. Technol.* **1997**, *31*, 289−295.

(36) Bradford, S. A.; Bettahar, M. Straining, attachment, and detachment of *Cryptosporidium* oocysts in saturated porous media. *J. Environ. Qual.* **2005**, *34*, 469−478.

(37) Redman, J. A.; Grant, S. B.; Olson, T. M.; Hardy, M. E.; Estes, M. K. Filtration of recombinant Norwalk virus particles and bacteriophage ms2 in quartz sand: Importance of electrostatic interactions. *Environ. Sci. Technol.* **1997**, *31*, 3378−3383.

(38) Church, S. E. *Geochemical and Lead-Isotope Data from Stream and Lake Sediments, and Cores from the Upper Arkansas River Drainage: Effects of Mining at Leadville, Colorado on Heavy-Metal Concentrations in the Arkansas River*; U. S. Geological Survey Open-File Report 93-534, U. S. Department of the Interior, U. S. Geological Survey: Denver, CO, 1993.

(39) Chen, J. Y.; Ko, C.-H.; Bhattacharjee, S.; Elimelech, M. Role of spatial distribution of porous medium surface charge heterogeneity in colloid transport. *Colloids Surf., A* **2001**, *191*, 3−15.

(40) Schijven, J. F.; Hoogenboezem, W.; Hassanizadeh, S. M.; Peters, J. H. Modeling removal of bacteriophages MS2 and PRD1 by dune recharge at Castricum, Netherlands. *Water Resour. Res.* **1999**, *35*, 1101−1111.

(41) Harvey, R. W.; Garabedian, S. P. Use of colloid filtration theory in modeling movement of bacteria through a contaminated sandy aquifer. *Environ. Sci. Technol.* **1991**, *25*, 178−185.

(42) Tufenkji, N.; Elimelech, M. Correlation equation for predicting single-collector efficiency in physicochemical filtration in saturated porous media. *Environ. Sci. Technol.* **2004**, *38*, 529−536.

(43) Kuznar, Z. A.; Elimelech, M. Adhesion kinetics of viable *Cryptosporidium parvum* oocysts to quartz surfaces. *Environ. Sci. Technol.* **2004**, *38*, 6839−6845.

(44) Medema, G. J.; Schets, F. M.; Teunis, P. F. M.; Havelaar, A. H. Sedimentation of free and attached *Cryptosporidium* oocysts and *Giardia* cysts in water. *Appl. Environ. Microbiol.* **1998**, *64*, 4469−4466.

(45) Bamford, J. K. H.; Bamford, D. H. Capsomer proteins of bacteriophage PRD1, a bacterial virus with a membrane. *Virology* **1990**, *177*, 445−451.

(46) Ranucci, L.; Muller, H. M.; Larosa, G.; Reckmann, I.; Morales, M. A. G.; Spano, F.; Pozio, E.; Crisanti, A. Characterization and immunolocalization of a *Cryptosporidium* protein containing repeated amino-acid motifs. *Infect. Immunol.* **1993**, *61*, 2347−2356.

(47) Parks, G. A. The isoelectric points of solid oxides, solid hydroxides, and aqueous hydroxo complex systems. *Chem. Rev.* **1965**, *65*, 177−198.

(48) Derjaguin, B. V.; Landau, L. Theory of the stability of strongly charged lyophobic sols and the adhesion of strongly charged particles in solutions of electrolytes. *Acta Physicochim. URSS* **1941**, *14*, 633−662.

(49) Verwey, E. J. W.; Overbeek, J. Th. G. *Theory of the Stability of Lyophobic Colloids*; Elsevier: Amsterdam, The Netherlands, 1941.

(50) Hahn, M.; O'Melia, C. R. Deposition and reentrainment of Brownian particles in porous media under unfavorable chemical conditions: Some concepts and applications. *Environ. Sci. Technol.* **2004**, *38*, 210−220.

(51) Tufenkji, N.; Elimelech, M. Breakdown of colloid filtration theory: Role of the secondary energy minimum and surface charge heterogeneities. *Langmuir* **2005**, *21*, 841−852.

(52) Bhattacharjee, S.; Ryan, J. N.; Elimelech, M. Virus transport in physically and geochemically heterogeneous subsurface porous media. *J. Contam. Hydrol.* **2002**, *57*, 161−187.